# A method for risk analysis of ship collisions with stationary infrastructure using AIS data and a ship manoeuvring simulator

N.B. When citing this work, cite the original published paper.

(article starts on next page)

# A method for risk analysis of ship collisions with stationary infrastructure using AIS data and a ship manoeuvring simulator

Axel Hörteborn [a,b,*], Jonas W. Ringsberg [b]

[a] *SSPA Sweden AB, SE-400 22, Gothenburg, Sweden*
[b] *Chalmers University of Technology, Department of Mechanics and Maritime Sciences, Division of Marine Technology, SE-412 96, Gothenburg, Sweden*

A B S T R A C T

The study presents a methodology that uses AIS data and a ship manoeuvring simulator to simulate and analyse marine traffic schemes with regard to risks for accidents. An event identification method is presented, which is needed for the accident scenario part of the methodology. This is based on AIS data, where the Great Belt VTS area was used to verify the methodology. Three events that could result in ship-bridge allisions were modelled and simulated in the simulator: drifting ship, sharp turning ship and miss of turning point. The Monte Carlo method was used to perform large number of simulator runs, including a parameter sensitivity analysis. The probability of a ship allision against the Great Belt Bridge was calculated to be 0.007. Analysis of the ship-bridge allision cases was shown to be dominated by the event drifting ship. This event has a relatively low kinetic energy at the impact, and the expected allision energy for a 1,000-year allision corresponds to a 178 m tanker with 57,870 DWT and ship speed 14.6 knots. Finally, this study presents a mitigation analysis, which shows how the probability of allisions can be reduced by reducing the ship speed or altering the traffic separation scheme.

## 1. Introduction

The advancement in bridge building engineering during the 20th century created an opportunity to build large bridges that span over wide waterways with intensive ship traffic. Risk analysis was used as the method to ensure that the bridge design and waterway traffic fulfilled expected safety standards. Despite this, 34 major bridge collapses occurred in the period from 1960 to 2007 that were caused by ship-bridge allisions (*def.*: ship collision with a bridge), which resulted in the loss of more than 340 lives (AASHTO, 2009). In addition to environmental and service loads that form the basis of the strength design of a bridge spanning over a waterway, the accidental probability of various hazardous events and accidental loads must also be considered.

In Europe, the norms and standards for all building codes are described in the Eurocode. In Eurocode 1, general equations are proposed for the calculation of accidental loads to be used in the design of bridges (CEN, 2006). For ship-bridge allisions, these equations are based on Eq. (1) with reference to the research presented by Fujii (1983) and Macduff (1974):

$$N_{Al} = N \times P_C \qquad (1)$$

where $N_{Al}$ is the number of allisions, $N$ is the number of ships and $P_c$ is the causation factor. There is limited guidance in Eurocode 1 on how the causation factor should be determined. Pedersen (1995, 2000) proposed that it can be estimated using the number of accidents (or allisions for ship-bridge contacts) divided by the number of ship passages. Since this approach relies on the number of reported accidents and traffic statistics in the area of interest, the accuracy of the value of the calculated causation factor depends on these data. Hassel et al. (2011) and Psarros et al. (2010) found that only approximately 50 percent of all accidents are reported in accident statistics databases, hence, the causation factor is underestimated (and, thereby, the probability of accidents).

This study presents a new methodology that handles the shortcomings in the determination of the causation factor in the risk analysis. It uses the approach proposed by Hollnagel et al. (2006) to identify scenarios that lead to accidents, together with AIS data, to calculate the probability of ship collisions with fixed infrastructure; this approach is applied in the study as ship-bridge allision. Hollnagel et al. (2006) proposed that there are different "layers" leading to an accident that should be assessed: root cause, event and the accident itself. For example, an officer on watch falls asleep [root cause], the ship continues past a turning point [event] and ultimately grounds [accident]. The

availability of AIS data in combination with the layer approach is the key issue in the methodology presented in this study.

Fujii (1983) and Macduff (1974) pioneered and established the basic theory for the current research field. At that time, AIS data were not available. The introduction and availability of AIS recordings have, according to Svanberg et al. (2019), resulted in new possibilities to enhance the accuracy in maritime risk assessments. AIS data are, therefore, used in this study for two purposes: to represent the real traffic statistics of ships passing a waterway; and to benefit from reverse engineering, where advanced numerical simulations are carried out to represent failure event statistics that are more valid compared to what has been reported (i.e. non-reported events and accidents can be captured and replicated).

Computer-based simulation models have been used in the maritime field for decades. One example is Källström and Ramzan (1985), who used a combination of simulation models and model tests to install the world's first commercial Tension Leg Platform. Nowadays, there are various types of maritime simulation models and software for different purposes. One simulation model that includes the [event] failure is the Maritime Transportation System (MTS) model. This model handles the ships' temporospatial positions in a time-domain simulation, but the hydrodynamic forces are not calculated, making it relatively fast and straightforward to use. This type of simulator was used by Uluscu et al. (2009), who studied the risk of accident in the Strait of Istanbul. van Dorp and Merrick (2011) proposed using the MTS model for risk assessments in coastal areas. In this model, the traffic was simulated on routes obtained from AIS data, and the ship failures and errors in the model were simulated based on expert opinions. Goerlandt and Kujala (2011) continued this research and implemented the DMTS model. This simulator is also based on AIS data, but it addresses the meeting situations differently. Goerlandt and Kujala (2011) used a Monte Carlo method to estimate the risk of collision and grounding in the Gulf of Finland. Rasmussen et al. (2012) used the ShipRisk software to quantify the risk to ship traffic in the Fehmarnbelt fixed link project. This software is a mixture of the models by Pedersen (1995) and an MTS simulator. In Rasmussen et al. (2012), the probability of human error, loss of propulsion, and steering machine failure were analysed.

The purpose of the study is to present new methodology using AIS data and a ship manoeuvring simulator to calculate the accident probabilities in marine traffic near bridges spanning over wide waterways. The methodology is verified in a case study on grounding accidents. Its wider applicability is presented in a demonstration study where the probability of ship-bridge allisions is calculated. With the proposed methodology, it can be numerically shown which ships and traffic situations that are over-represented in failure event analyses; hence, mitigation actions can be proposed that reduce the risk of accidents. It can also be used to identify candidate ships that should be used as "target" ships in bridge concept designs, to ensure sufficient bridge structural strength that can withstand the kinetic energy impacting the bridge; see Sha and Amdahl (2019).

In the proposed methodology, there is no equation that estimates the number of allisions; this is the major difference compared to methods based on Eq. (1). The number of simulations is calculated by equations, but the simulations give the number of allisions. Another difference compared to previous research is that the methodology includes methods to obtain location-specific failure events regarding both duration and frequency. The proposed methodology can thus be applied to study risk mitigation options in location-specific areas. Note, however, that a limitation is that only single ships can be studied in each simulation. This is because the event statistics are gathered from single-ship situations, and it is challenging to model all human decisions that could be made in an autopilot logic. Apart from the probability of allision, the methodology also enables estimations of the design energy the structure needs to withstand. This is possible since the kinetic energy just before the allision is captured for all simulated allisions.

The remainder of the paper is structured as follows. Chapter 2 presents the overall methodology, including a brief description of the ship manoeuvre simulator. Chapter 3 introduces the simulation scenarios in the study, which have been defined for verification and demonstration purposes of the methodology. The event statistics used in these scenarios are presented in Chapter 4. A presentation of the simulation setup in the ship manoeuvre simulator are presented in Chapter 5 together with the case study area, followed by results and discussions of the analyses in Chapter 6. The conclusions are presented in Chapter 7.

## 2. Methodology

The methodology in the study integrates modern simulation and analysis tools to ensure safe and robust designs when new bridges that span over waterways are built. It should be noted that it can also be used to assess existing bridges if they fulfil today's design and safety criteria, or if mitigation actions need to be activated. This is justified since the majority of the bridges that exist were built several decades ago. They were designed based on the marine traffic that was present at that time, considering an extrapolation of its increase and the ideas of which ships that would be built in the future. It is likely that the assumptions that formed the basis for safety factors in the bridge design are not aligned with today's marine traffic situation and sizes of ships. One similar example where the design criteria had become obsolete is the design of the twin towers of the World Trade Centre in New York (USA) and the attack they were subjected to on September 11, 2001. The two towers were designed and constructed in the 1960s to withstand an airplane crash. However, 40 years later, both the size of the aircrafts and the amount of fuel they carry had increased significantly more than expected in the scenarios they were designed to withstand (El-Naby et al., 2014).

The methodology in this study has three major parts: collection of AIS data, analysis of AIS data for event definition and modelling, and modelling and simulation of events in a ship manoeuvre simulator. The AIS data are used to collect both event and general traffic statistics. Based on the event statistics, different event models are proposed to be used as input to the simulator, where the evolvement of events is simulated and analysed. It should be noted that one advantage of using a ship manoeuvre simulator is that not all of the events that are introduced or triggered actually lead to an accident. The simulator can thus help us to understand why some events did not result in an accident. It can be used in investigations as forensic analysis of accidents that actually happened, or it can be used to simulate and analyse the consequence of mitigation actions. A schematic of the methodology is shown in Fig. 1; see Chapter 3 for more details how the AIS data are investigated and Chapter 5 for more details and a presentation of the simulation setup in Fig. 7.

### 2.1. Ship manoeuvre simulator

The SEAMAN ship manoeuvre simulator, which was developed by SSPA (http://www.sspa.se), was used in this study. The simulator is a software code where the ship's motions are modelled in all six degrees-of-freedom. It is a module-based software where the definition of the ship model's characteristics is divided into subsystems, e.g. the hull, engine, propeller and rudder. The simulator includes spatial-temporal subsystems and numerical codes that calculate the forces acting on the ship that are induced by the wind, waves and currents; shallow water and bank effects are also considered (Andreasson et al., 2005; Ottosson and Bystrom, 1991). Total force equilibrium of the ship model is solved in a nonlinear mathematical model in every time step according to a procedure presented in Ottosson (1994).

A SEAMAN ship model requires several hundreds of parameters to accurately represent a ship and its characteristics in the simulator. A ship's hydrodynamics and resistance properties can be fine-tuned if test data are available from model testing. When new models are defined in the simulator, a procedure for parameter sensitivity study of the ship
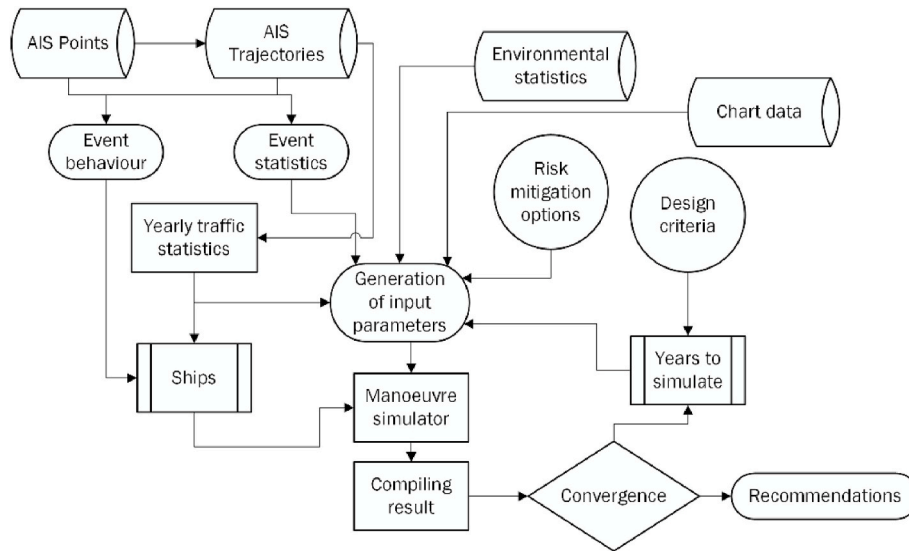
**Fig. 1.** Schematic of the methodology presented in the study.

model's parameters is always carried out. For example, to ensure that the manoeuvrability of the ships used in this study was correctly modelled in SEAMAN, each ship model was simulated and verified against the zig-zag and turning circle tests from the IMO's "Standards for ship manoeuvrability" (IMO, 2002). Running these tests in a simulation context have also been applied by others like Budak and Beji (2020), who used the tests to ensure the ship's manoeuvrability while implementing a course-keeping autopilot.

Fig. 2 presents a screen shot from a simulation when the simulator is run in desktop mode in real time. It can also be run in batch mode with an autopilot navigating the ship according to a pre-defined route, failure

event or simulation scenario determined by the user. The batch mode was used in this study since it significantly reduced the simulation time and there was no need to survey the simulations in real time on a screen. It was also a necessity because of the large number of simulations carried out using the Monte Carlo method; see Chapters 5 and 6.

## 3. Definition and identification of failure events using AIS

Simulation and analysis of ship accidents and their causes can be carried out in multiple ways. Pedersen (1995, 2020) proposed a method based on the work of Fujii (1983) and Macduff (1974). In this method,
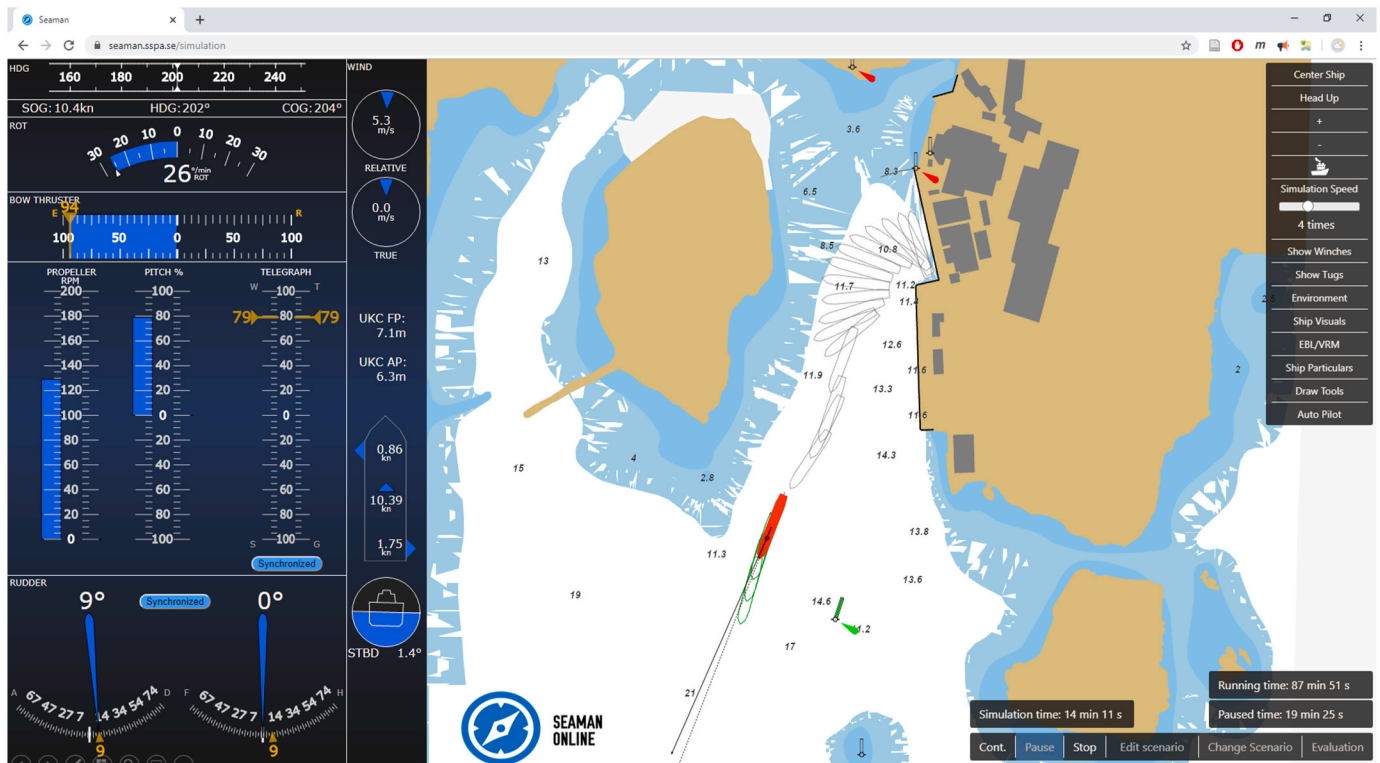


**Fig. 2.** Example from a SEAMAN simulator run in desktop mode (screen shot). It shows the history of the ship's manoeuvres when it leaves the port and its navigation trajectory when it enters the fairway.

situations are defined that can result in an accident, an approach that has been applied by among others Montewka et al. (2012) and Goerlandt and Kujala (2011). Pedersen's situation-based approach can be efficiently used in mathematical models that do not involve or need a ship manoeuvring simulator or detailed modelling of the ship's motions and dynamics. However, one shortcoming is that it relies on historical events/accidents and data for known traffic situations and ships, which often are related to very low probabilities, and, hence the method is sensitive to the access to and quality of data (Chen et al., 2019). The advantage of the approach is that analyses can be made with low modelling and computation efforts, which often are suitable in risk analyses that involve the Monte Carlo method.

The ship manoeuvre simulator presented in Chapter 2 was used in this study instead of Pedersen's approach. The advantage of the simulator approach is that it opens up new possibilities to simulate, assess and execute risk analysis of existing and future marine traffic situations that may involve infrastructure offshore. The gain of this approach is that specific details of the trace from event to accident can be obtained and analysed. This includes data of ship types, weather situations, ship operation profiles, fairway layouts and infrastructure objects, which can be modelled and systematically varied in parametric studies; it does not need an explicit value or expression of the causation factor, which is required in Pedersen's approach. The drawback is that it requires some more modelling and computation efforts, but the simulator software used in this study offers batch mode simulations to overcome the challenge. In addition, instead of defining and analysing accidents, three types of events are identified in the study as relevant and critical for ship-bridge allisions in relatively narrow waterways: drifting of the ship, sharp turning of a ship and miss of a turning point. They are similar to the categorisation presented in Uluşçu et al. (2009), van Dorp and Merrick (2011) and Rassmusen et al. (2012); see a discussion in Chapter 6.4 for other types of events.

The AIS data of the marine traffic in the area are needed to model, simulate and analyse the events. Since 2002, ships larger than 300 gross tonnes must have an AIS transponder, which means that this information has been available after 2002. AIS messages are separated in two message types: position report and metadata message (Raymond, 2019). At sea, every ship issues a position report every 2–10 s, depending on the ship's speed and turning rate. In this study, this information is handled both as "single points" and after post-processing as "trajectories", defined by multiple points and represented by lines connecting similar points. The trajectories then contain data from both the position reports and the metadata messages data and are stored in a PostgreSQL database with the spatial extension PostGIS. For more details about how the trajectories were constructed with a Douglas-Peucker compression, see Hörteborn et al. (2019) or a similar method presented in Zhao and Shi (2019) and Wei et al. (2020).

The following subchapters present how AIS data were used to quantify frequencies and durations for the three events of drifting ship, sharp turning ship and miss of turning point. Each subchapter ends with a summary of how the simulation of the event was implemented in the simulator's autopilot. In short, the event identification using AIS data was carried out in two steps. First, an automatic filter with specified conditions that helped define an event was applied to the AIS trajectories, followed by a second manual step applied to the remaining tracks that could not be identified as a clear event among the three categories. Events identified by the AIS data were also used in the process of calibrating the autopilot's behaviour, for example, related to the time to turn off the steering system and lock the rudder's position.

### 3.1. Event "drifting ship"

The drifting ship event is defined as a ship that appears to drift with the waves, the wind and the current with no possibility to turn on its engine. It is assumed that the probability that the drifting ship event will occur is the same along the fairway; see Furnes and Amdahl (1980),

Rasmussen et al. (2012) and Kaneko (2012).

The AIS data were used to identify drifting ships by following the AIS trajectories and applying the following criteria as filters:

- speed over ground (SOG): should be less than 2 knots.
- course over ground (COG): should differ more than $20°$ from the heading.
- duration: longer than 5 min.

Each candidate ship that fulfilled these criteria was manually checked to ensure that there were no obvious reasons for their drifting behaviour, which would then result in the candidate being removed from the sample. Examples of such candidates that should be excluded as drifting ships are slow steaming ships and ships that intervene with other ships, e.g. ships that pickup pilots or change crew. The duration of the event for a drifting ship was defined by the position report where the ship started to lose speed (or its last known position) to the position report where the ship recovered control and started to either pick up speed again or anchored.

In the simulator, a drifting ship is modelled as fully operational for the first 60 s in a simulation case whereafter the propulsion system is turned off. At this instant, the ship begins to lose speed, and the autopilot tries to keep the ship's course on track for as long as possible. This setup correlates with the most common ship behaviours from AIS data observations from the ship traffic studied in Chapter 4; complete blackout (including the steering engine) was not observed. The simulation in the simulator continues for the duration of the event, which can either be the duration as measured from AIS data (see above), from a pre-defined time by the user when the propulsion system is turned on again, or when the ship is anchored. In this study, the first option was used. Fig. 3 shows an example from a comparison of results from a simulator simulation (green ship contours) and the real AIS track (grey ship contours) for the same case of a drifting ship. This example shows that the simulator almost replicates the AIS track.

### 3.2. Event "sharp turning ship"

The sharp turning ship event is defined as a ship that may suffer from a malfunction in the rudder giving rise to a locked rudder that turns the ship distinctly to starboard or port; see Pedersen et al. (2020) for the category III type of accident for a similar situation or event. In the current study, it is assumed that when this event occurs, the ship decreases its speed to gain time to repair/fix the rudder problem. When the ship's speed decreases, and there is no rudder effect that can be controlled by the crew, it looks as if the ship is drifting in the AIS data. Thus, the principles and filters used to identify drifting ships can initially be applied to identify candidates for the current event. To distinguish this event from the event drifting ship, the following complementary criteria are used:

- a ship that continuously loses its speed, without an instant sharp turn, is categorised as a candidate for the event drifting ship.
- a ship that starts its drifting with an instant turn and has a rudder malfunction is categorised as a candidate for the event sharp turning ship.

The duration of the sharp turning ship event for a ship was defined by the position reported where the ship started to turn sharply, to the position reported where the ship recovered control and started to either pick up speed again or anchored.

Modelling this event in the simulator is challenging, since, in reality, the crew of a ship will react and act differently in each scenario to a malfunction of the rudder. Nevertheless, the simulator setup to simulate this event is in the study is defined as a fully operational ship the first 60 s of the simulation case whereafter the rudder is set to either full starboard or full port. After another 60 s in the simulation, the engine is
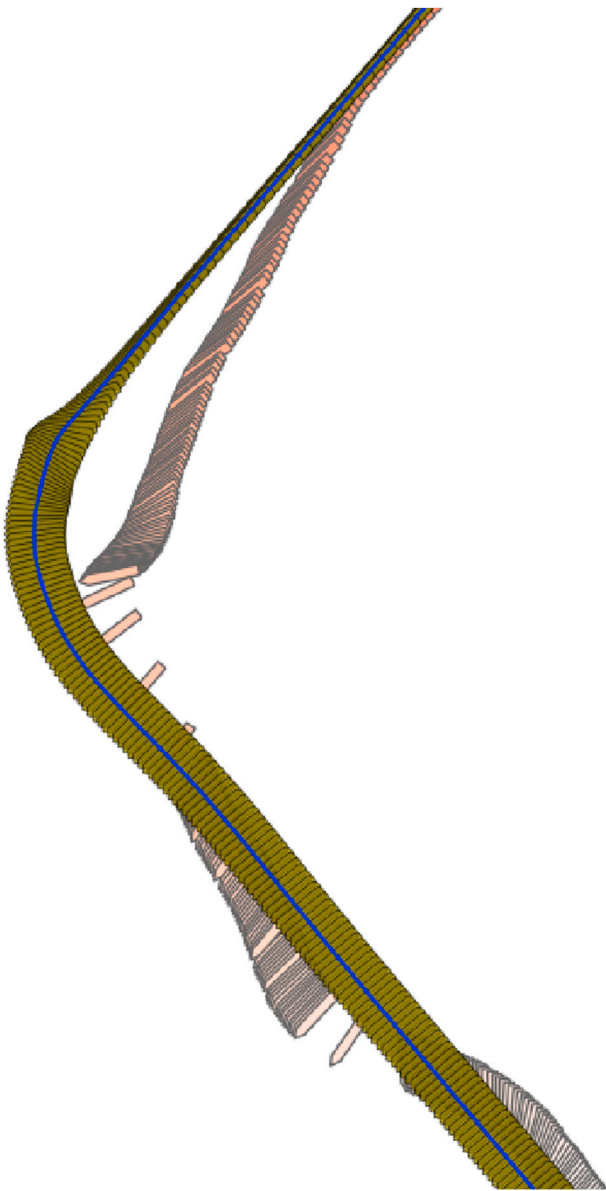
**Fig. 4.** Sharp turning ship: simulated track (contours plotted in green, one position every 20 s connected with a blue line) overlaid the real AIS data (contours plotted in red). (For interpretation of the references to colour in this figure legend, the reader is referred to the Web version of this article.)

(2020) for the category II type of accident for a similar situation or event. The event is exemplified in Fig. 5, where the blue line shows a ship (traveling from south west to north east), failing to follow the expected/normal traffic behaviour. The ship passes through the border (line 3) of the Traffic Separation Scheme (TSS). After some time, the "mistake" is observed, and the ship turns back to the main navigation lane of the fairway. The reason for the occurrence of this event can have various root causes, such as fatigued crew (falling asleep), rudder stuck mid ship, human errors during navigation, etc.

The AIS data were used to identify miss of turning point ships by following the AIS trajectories and applying the following criteria as filters, here presented related to the example in Fig. 5:



**Fig. 3.** Drifting ship event: simulated track (contours plotted in green, one position every 20 s connected with a blue line) overlaid the real AIS data (contours plotted in grey). (For interpretation of the references to colour in this figure legend, the reader is referred to the Web version of this article.)

turned off, and after another 5 min, the rudder is assumed functional again and set to mid ship position. This sequence, times and behaviours were determined from the authors' experiences from analyses of AIS data, parametric studies in the simulator and attempts to mimic real events in the simulator's environment. Fig. 4 shows an example from a comparison of results from a simulator simulation (green ship contours) and the real AIS track (red ship contours) for the same case of a sharp turning ship. The turn is initiated with constant speed, indicating that it is a sharp turning point event and not a case of loss of propulsion (i.e. drifting event). This example shows that the simulator almost replicates the AIS track for this event.

### 3.3. Event "miss of turning point"

The miss of turning point event is defined as a ship that continues straight ahead, passing a marked or expected turning point, but manages to correct its course later to the main navigation lane; see Pedersen et al.
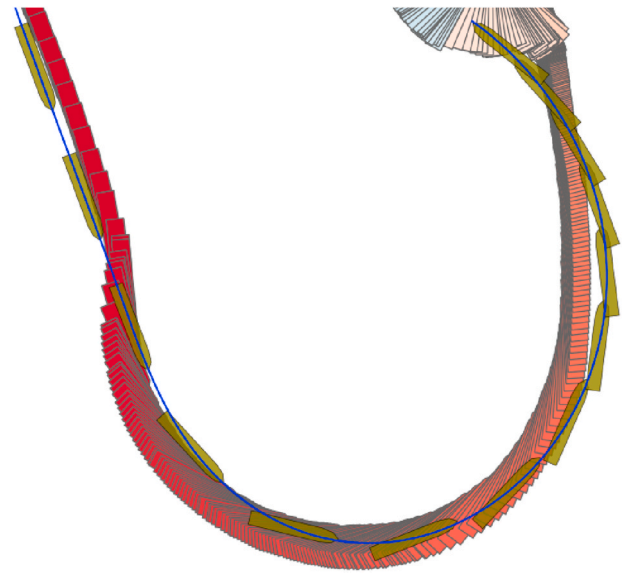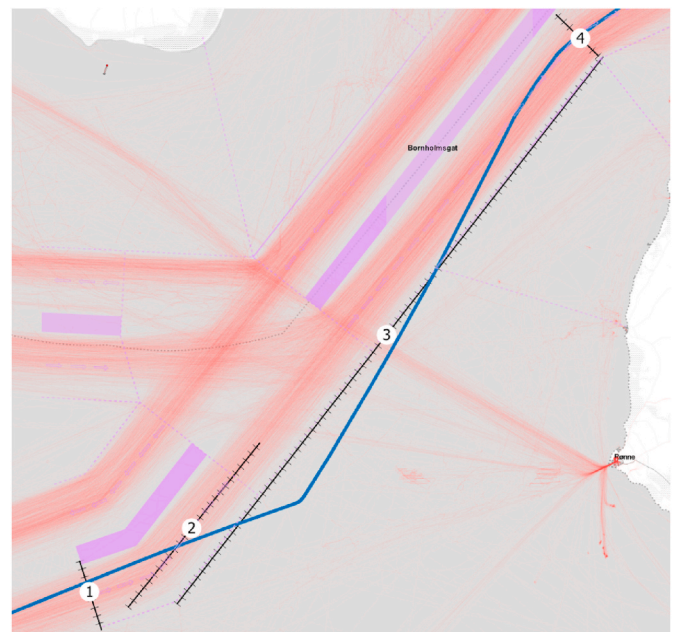


**Fig. 5.** An example of a ship that fails to turn at a marked turning point; the example is taken from the TSS Bornholmsgat area.

- the ship should cross the pre-defined TSS border lines, i.e. the border lines 1, 3 and 4 in Fig. 5.
- the COG should differ less than 5° between the crossing of lines 1 and 3.
- the SOG should differ less than 1 knot between the crossing of lines 1 and 3.

Similar to the other event categories, every ship that fulfilled these criteria was manually checked to ensure that there were no obvious or other reasons for its behaviour and choice of path. For example, a ship with a distance smaller than its own ship domain to another ship was excluded, since its path could have been affected by the other ship (i.e. intentional and voluntary miss of turning point to avoid an incident). The definition of the size of the ship domain followed the method presented in Hörteborn et al. (2019).

The duration of the miss of turning point event for a ship was defined by the position of the expected turning point and the position reported where the ship actually turned. The expected turning point here is the point where the majority of all ships turn to follow the TSS; see line 2 in Fig. 5, which marks when ships are supposed to make the turn in the example.

Modelling this event in the simulator was done in the case study as follows. The ship is run as expected during the initial 2 min of the simulation in order to ensure that it is on the correct navigation path. After that, the autopilot is turned off, and the rudder is locked in midship position and remains so for the remaining time duration of the event.

## 4. Event statistics

This chapter present event statistics and durations for the events defined in Chapter 3. The case study presented in Chapters 5 and 6 emphasises the Great Belt VTS area. However, in this chapter, the statistics and analyses of the TSS Bornholmsgat area and the results reported in Rasmussen et al. (2012) are included for comparison purposes.

The AIS data were based on the marine traffic in the Great Belt VTS and TSS Bornholmsgat areas during the period 2014 to 2019 obtained from DMA (2020). The data were analysed with the methodology presented in Chapter 3. Rasmussen et al. (2012) presented their results for "human failure" in the Kadetrenden area using AIS data from 2007 to 2010, and their statistics for "loss of propulsion" and "steering machine failure" were based on four years of incident reports from the Great Belt VTS.

### 4.1. Event frequencies

It assumed that the probability of occurrence and the duration of the events defined in Chapter 3 are independent of ship type and size. In total, 153 events were identified in the Great Belt VTS and TSS Bornholmsgat areas using the event identification methods described in Chapter 3. Table 1 presents a summary of the number of events for each event category, together with the number of sailing hours that were used to identify the "drifting ship" and "sharp turning ship". Two waypoints in these areas were used to define the event "miss of turning point", and the number of turns at these waypoints are also presented in the table. The frequency for "drifting ship" and "sharp turning ship" was

**Table 1**
Number of events, hours and turns in respective area.

| Data analysis | Great Belt VTS | TSS Bornholmsgat |
|---|---|---|
| Number of drifting ship events | 34 | 65 |
| Number of sharp turning ship events | 2 | 5 |
| Number of sailing hours | 522,296 | 713,531 |
| Number of miss of turning point events | 19 | 26 |
| Number of turns at waypoints | 122,319 | 124,705 |

calculated by dividing the number of events with the number of sailing hours. The "miss of turning point" frequency was calculated by dividing the number of events with the number of ships making the turn. These frequencies together with the data from Rasmussen et al. (2012) are shown in Table 2.

The event frequency for "drifting ship" is in same order of magnitude in the three studies. The values for the Great Belt VTS and Rasmussen et al. (2012) show very good agreement; thus, the method described in Chapter 3.1 for this event was considered verified. The lower value for the Great Belt VTS area compared to the TSS Bornholmsgat area is due to the ships in the former area being able to manoeuvre more easily and safely and anchor outside the fairway if they experience minor trouble, such as a partial blackout. It should be noted that with the event identification method presented in Chapter 3.1, it is not possible to differentiate these events from planned anchoring. In the case study in Chapter 5, simulations and analyses of the Great Belt VTS area, this event's frequency was set to $0.65 \times 10^{-4}$/hour.

The event frequency for "sharp turning ship" differs some between the different studies. However, only two cases were identified for the two studies in the Great Belt VTS area, which are too few to rely on when generating statistics. It was assumed that the value of this event's frequency should be somewhat lower than the average value from the three studies, it was set to $0.070 \times 10^{-4}$/hour. A sensitivity analysis in which this event's frequency is increased 50 percent is presented in Chapter 6.4.

The event frequency for "miss of turning point" shows relatively good conformity between the three studies; the value from Rasmussen et al. (2012) is, instead of calculating the event frequency in terms of occurrences per turn, based on "human failure" and event frequency per hour as the unit. Based on the same reasons as for the "drifting ship" event, an event frequency of $1.55 \times 10^{-4}$/turn was used in the simulations and analyses in Chapter 5. However, it should be noted the duration time of the event was found to be notably different between these three studies, see the following chapter for the analysis.

### 4.2. Event durations

The definition of the duration of each event was defined in Chapter 3. Fig. 6 presents a summary of the durations for the "drifting ship" and "sharp turning ship" event categories. The symbols in the figure represent results from the AIS data processing, while the lines represent fitted curves according to the distributions presented in Table 3. For the former category, the results are presented separately for the Great Belt VTS, the TSS Bornholmsgat and Rasmussen et al. (2012). For the sharp turning ship event, there were too few cases in the Great Belt VTS and the TSS Bornholmsgat areas to make a distribution. To overcome this was six event durations from a third area, the Kiel Canal, included to make this distribution (this area is discussed in Chapter 6.5). However, the event had similar durations in all areas, so they were fitted to one common distribution representing the event.

The results in the figure show that the duration of the drifting ship event is the shortest in the Great Belt VTS area. It can be explained by the fact that this area offers the best opportunity to anchor. The event

**Table 2**
Summary of event frequencies where * refers to "loss of propulsion", ** to "steering machine failure" and *** to "human failure" in Rasmussen et al. (2012).

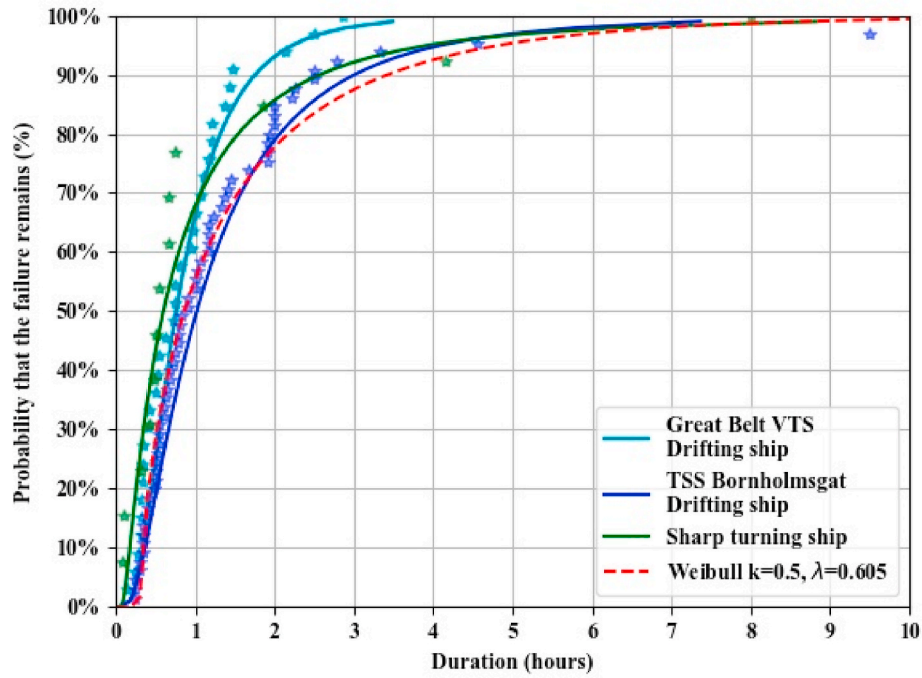| Event category | Great Belt VTS | TSS Bornholmsgat | Rasmussen et al. (2012) |
|---|---|---|---|
| Drifting ship | $0.65 \times 10^{-4}$/ hour | $0.91 \times 10^{-4}$/hour | $0.6 \times 10^{-4}$/hour* |
| Sharp turning ship | $0.038 \times 10^{-4}$/ hour | $0.092 \times 10^{-4}$/ hour | $0.1 \times 10^{-4}$/hour** |
| Miss of turning point | $1.55 \times 10^{-4}$/ turn | $2.10 \times 10^{-4}$/turn | $2.5 \times 10^{-4}$/hour*** |

**Fig. 6.** Duration of the events drifting ship (individually: Great Belt VTS, TSS Bornholmsgat, Rasmussen et al. (2012)) and sharp turning ship (summary of all: Kiel Canal, Great Belt VTS, Bornholmsgat TTS). The dots represent the measurements, and the lines are the result of the curve fitting presented in Table 3.
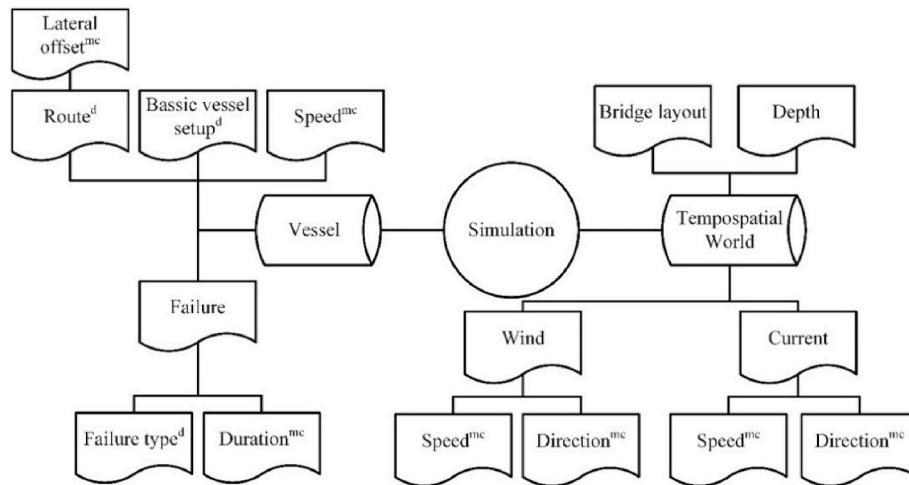


**Fig. 7.** Schematic of deterministic (d) and randomly generated (mc) parameters in the SEAMAN simulator simulations.

**Table 3**
Statistical distributions and their parameters for duration of events (time in hours). The parameters correspond to σ = standard deviation, ι = location, λ = scale and μ = mean value.

| Event category | Great Belt VTS | TSS Bornholmsgat | Rasmussen et al. (2012) |
|---|---|---|---|
| Drifting ship | Lognormal $\sigma = 0.71$ $\iota = 0.021$ $\lambda = 0.69$ | Lognormal $\sigma = 0.87$ $\iota = 0.1$ $\lambda = 0.97$ | Weibull $\sigma = 0.5$ $\lambda = 0.605$ |
| Sharp turning ship | Lognormal: $\sigma = 1.2$; $\iota = 0.06$ $\lambda = 0.54$ | | n/a |
| Miss of turning point | Normal $\mu = 0.064$ $\sigma = 0.015$ | Normal $\mu = 0.19$ $\sigma = 0.047$ | Less than 0.33 |

category "miss of turning point" is not included in the figure, but its statistical distributions are presented in Table 3.

### 4.3. Accident statistics in the areas

Collection of accident statistics in the Great Belt VTS area was emphasised since this area was used in the simulator case study in Chapter 5. Three sources were used to ensure that the majority of accidents reported between 2010 and 2019 in the area were collected. In the accident records of IHS Fairplay (2020), five strandings, two collisions, one contact and one fire accident were reported. In addition to these accidents, the Norwegian Maritime Authority (Sjofartsdirektoratet, 2020) reported one fire accident, and no additional accidents were found reported in the EMCIP database (EMCIP, 2020).

## 5. Description of simulator simulations and case study

The chapter presents a case study where the SEAMAN simulator was used to simulate and analyse the marine traffic situation in the Great Belt VTS area. Chapter 5.1 presents how the simulator simulations were planned and setup followed by specific details and descriptions of the case study in Chapter 5.2.

### 5.1. Simulator simulations and setup

The simulations in the SEAMAN simulator were run in sets, where each set contained 90 batches of simulations. The 90 batches were based on three event categories, 15 types of ships and two directions of ship routes; see Chapter 3 for event categorisation and Chapter 5.2 for ship types and route directions specific for the case study marine traffic situation.

The number of simulations in each batch, for the drifting ship and sharp turning ship events, was calculated using Eq. (2):

$$N_{Sim,i} = \sum_{j=1}^{15} \sum_{k=1}^{2} P_{ft,i} \times N_{Cat,jk} \times t_{N,jk} \times Y_R \quad (2)$$

where $N_{Sim,i}$ is the number of simulations for event $i$ (1 = drifting ship; 2 = sharp turning ship), $P_{ft,i}$ is the event probability per hour for the event under study (see event frequency in Chapter 4.1), $N_{Cat,j,k}$ is the estimated number of ships per year for ship type $j$ on a route $k$ in the area, $t_{N,j,k}$ is the average time ship type $j$ sails on the route $k$, and $Y_R$ is the number of repetitions of one year's traffic the simulation should represent.

The starting position of a ship in a simulation for an event varied between the simulations. It was assumed that the starting position of a ship (i.e. its position in the fairway when the simulation starts) follows the traffic separation scheme and spatially follows an even distribution along the route. The distance between starting positions, $D_{sp,ijk}$, was calculated according to Eq. (3), where $N_{Sim,i}$ was calculated according to Eq. (2), where $L_{r,k}$ is the length of the simulated route.

$$D_{sp,ijk} = L_{r,k} / N_{Sim,i}. \quad (3)$$

The number of simulations in each batch for the miss of turning point event ($i = 3$) was calculated using Eq. (4):

$$N_{Sim,i} = \sum_{j=1}^{15} \sum_{k=1}^{2} P_{CSA,i} \times N_{Cat,jk} \times N_{T,jk} \times Y_R. \quad (4)$$

where $P_{CSA,i}$ is the probability that a ship misses a turn, and $N_{T,jk}$ is the number of turns the ship $j$ makes on its route $k$. According to Chapter 3.3, these simulations started 2 min prior to the point where the turn was missed; a turning point was laterally distributed in accordance with their unique route.

The majority of the simulator simulations ended without ship grounding or ship-bridge allision. However, for the simulations that ended with an allision, the allision energy was calculated according to Eq. (5), where $M$ is the ship's displacement, $v$ the ship speed and $E$ is the allision energy. Note that this is the largest theoretical energy that may cause damage to the ship and the bridge structures, since the formula is simplistic it does not include detailed energy distribution which could be studied by external dynamics simulations; see Yu et al. (2016) and Lu et al. (2016).

$$E = (Mv^2)/2 \quad (5)$$

A central part of the presented methodology is the bridge design criteria. According to Johansen and Askeland (2019), there are different ways to interpret these criteria where the authors proposed to use of an FN-curve to better represent both the probability and the consequence. In this study, a risk criterion with a threshold of $1 \times 10^{-3}$ was selected, which means that a bridge struck by a ship should withstand and survive allisions with a probability level of $1 \times 10^{-3}$. The procedure to identify ships that follow this criterion was as follows. The allision energies from a complete simulation set in the simulator were sorted from the highest to lowest. The probability for the worst allision in the same set of simulations is then $1/Y_R$, and the second worst (or worse) has a probability of occurring $2/Y_R$. For this analogy, with simulator simulations of $Y_R = 10,000$ times, the 10th worst allision corresponds to the worst allision that has the highest probability to occur in 1,000 years. If $Y_R$ is increased to 100,000, the 100th worst allision corresponds to the allision energy with a probability to occur corresponding to $1 \times 10^{-3}$.

The SEAMAN simulator has two major parts in the simulator model: a model of the ship and a model of the environment (called "world"). Fig. 7 presents a schematic of the parameters of these models that have either been deterministic, $d$, or randomly generated, $mc$, in Monte Carlo simulations. The deterministic parameters were the three batch parameters (i.e. event categories, ship types and direction on route), and the seven randomly generated parameters were described by statistical distributions.

### 5.2. Case study: the Great Belt VTS area

The chapter presents the case study area in detail. It is presented from which the values and settings of the parameters lateral offset, route, ship, ship speeds and environmental variables were collected. The properties of the events were presented in Chapter 3 and their durations in Chapter 4.2.

The Great Belt VTS was chosen as the case study area since it has been studied by other researchers from a ship-bridge allision perspective; for an example, see Gluver and Olsen (1998). According to statistics in accident databases, numerous groundings in the area have been reported during the past few years (EMSA, 2019), and historic AIS data are available for the area (DMA, 2020). Fig. 8 presents a map of the marine traffic passing the area, and Fig. 9 presents histograms of the distribution in ship length, ship speed and lateral distribution for the marine traffic that passed the Great Belt Bridge during 2019. The marine traffic is spread laterally over the fairway, which, according to IALA (2014), can be represented by the normal distribution. In this study, this distribution is checked/updated at every waypoint for all traffic in 2019 since the properties of the distribution may vary in the fairway (here, called offset). By means of the offset (normal) distributions, indicated as Lateral offset$^{mc}$ in Fig. 7, a unique route could be generated for each simulator simulation.

Most of the traffic that passes the area follows the south-north T-route. It is divided into a deep water route and a normal route, see Fig. 8. Statistics of the marine traffic in the area during 2019 shows that 19,507 ships passed under the Great Belt Bridge, divided into 7,225 general cargo ships, 5,242 tanker ships, 2,094 RoPax/RoRo ships, 1,488 container ships, 1,484 bulk carriers and 1,974 unknown ship types. The length distribution of each ship type is presented in Fig. 10.

The results in the figure were used to define 15 representative ships in the simulator that together reflected the marine traffic in the area during 2019. Table 4 presents some of the ships specifics, ship speed (normally distributed, Speeds$^{mc}$ in Fig. 7) and the number of ships going north and south ($N_{Cat}$ in Eqs (2) and (4)). The three largest ships with regards to draught—Bulk, 226 m; Tanker, 241 m; Tanker, 260 m—used the deep water route in Fig. 8; all other ships use the normal route.

### 5.3. Metocean statistics for the Great Belt VTS area

The metocean statistics for the area were downloaded from the Copernicus Marine Service (2020). The wind statistics for the period 2015 to 2020 are presented in Fig. 11 as a wind rose plot for the location latitude $55.25°$ and longitude $11.0°$. The current statistics for the period 2016 to 2020 are presented in Fig. 12 as a current rose plot for the location latitude $55.2°$ and longitude $11.0°$. The data in the rose plots are used to define the wind and current loads in the simulator model; see
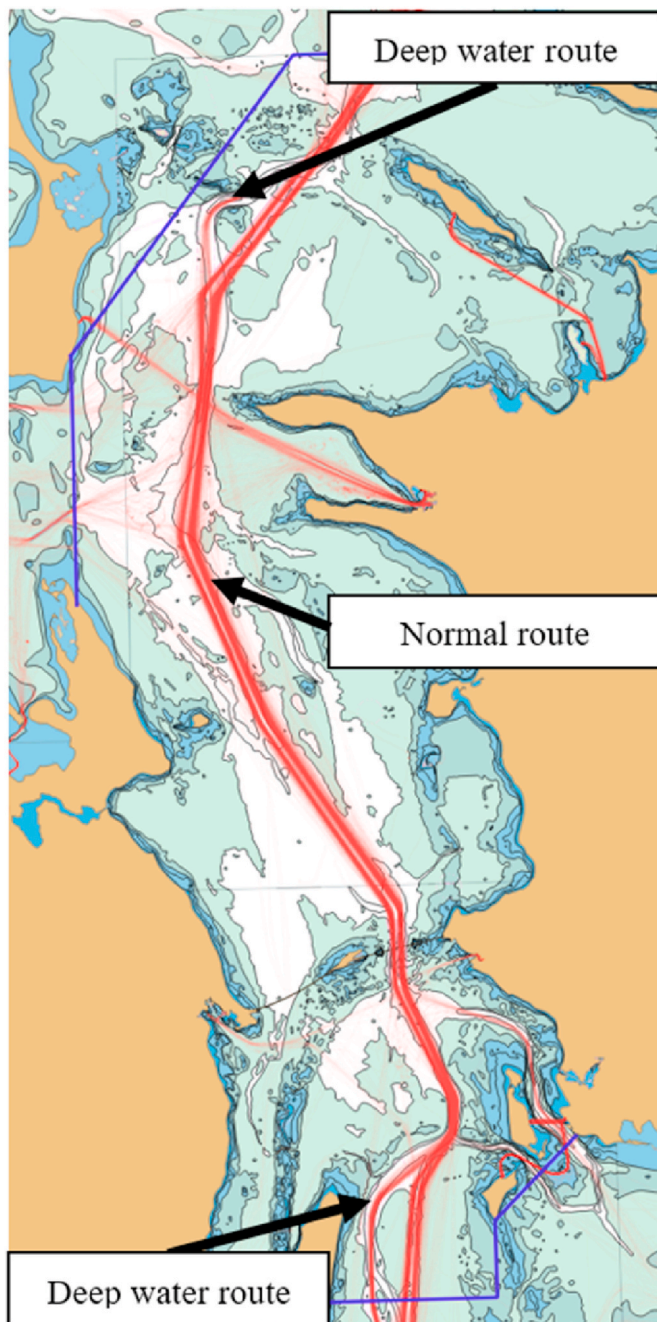
**Fig. 8.** Map presenting the marine traffic in the Great Belt VTS area.

Fig. 7.

The length of a colour bar in Fig. 11 indicates the probability of a specific wind speed and wind direction. For example, the wind directions around 11 percent of the time are from the south-west, where the wind speed is 2.5 percent of the time less than 3 m/s, 6 percent of the time between 3 and 6 m/s, 3 percent of the time between 6 and 9 m/s, and less than 0.5 percent of the time it is faster than 9 m/s. The wind rose plot in Fig. 11 shows that the dominant wind directions are from the west and the south-west, and that the wind speed is often below 9 m/s. Wind speeds larger than 9 m/s come from the west and sometimes from the east, but rarely from other directions. The current rose plot in Fig. 12 shows that there are currents in the area that are dominated by the directions north north-west and south south-east.

Forces from secondary waves induce drift forces on ships, and waves up to 2 m have some effects on a ship's manoeuvrability (Chillcce and el

Moctar, 2018). The probability to encounter different wave heights in the range 0–2.5 m in the area is presented in Fig. 13. This figure show that the probability to encounter waves larger than 1.5 m is very low, i.e. waves have a minor effect on a ship's manoeuvrability in the area. Hence, it was assumed that waves could be disregarded in the simulator model, which also reduce the computational efforts (less simulation time). To conclude, the influence from wind and current have a great effect on the drift force, and, hence, they were included in the simulator model, which, in this study, was defined as a four degrees-of-freedom ship model (heave and pitch were not considered).

## 6. Results

The simulator runs were defined in three categories divided into ten simulation sets for (i) investigation of the influence from random seeds in the generation of random variables, (ii) a sensitivity study of the parameters, and (iii) demonstration of examples of risk mitigation; see Table 5 for an overview of all simulation sets. The simulation of a single ship's voyage took approximately 2 s on an Intel Core i7-2600 3.4 GHz processor with 16 GB RAM memory and 64Bit architecture. One set of simulations consist of some four million ship voyages, which needed approximately 80 h to complete using eight processors.

The three sets, 1A, 1B and 1C, relate to the random seed study. They have the same input, but the random seed for the generation of random variables (*mc* in Fig. 7) is varied, which resulted in different values of the random variables. Hence, by defining the random seed, a simulation could be reproduced, ensuring that new combinations of random variables were generated (Harris et al., 2020). The number of simulations needed in the set was determined by a criterion defined in this study stating that the difference in allision energy between the simulation sets should not differ more than five percent.

The five sets in 2–4 in Table 5 were defined for sensitivity study analysis purposes in which the probabilities and duration time of the events were studied. The input data were based on the TSS Bornholmsgat area. One set investigated the increased probability and duration time of the event drifting ship, and another set investigated a fifty percent increase in probability of the event sharp turning ship. The miss of turning point event was separated into three sets: increase of both probability and duration time, increase of only the probability and increase of only the duration time.

Sets 5 and 6 were defined and used in examples of risk mitigation to demonstrate how the methodology presented in the study can be utilised. In set 5, a speed limitation of 12 knots was enforced, and in set 6, the navigation path was altered to force the traffic to navigate 2.6 nautical miles straight prior to the Great Belt Bridge instead of 1.6 nautical miles, which is the normal navigation path.

### 6.1. Analysis of the number of simulated traffic years ($Y_R$)

Sets 1A, 1B and 1C were used to investigate how many traffic years ($Y_R$) need to be simulated according to the discussion in Chapter 5.1. Table 6 presents the results from the simulator simulations with $Y_R = 10,000$ traffic years (or repetitions of one year). There is a difference in the number of groundings and allisions because of the different random seeds, which also affects the maximum allision energy and the 1,000-year allision energy for each simulation set. As described in Chapter 5.1 the 1,000-year allision energy represents the worst allision that has a probability of $1 \times 10^{-3}$ to occur. Because the 1,000-year allision energy differs more than 30 percent between the sets, $Y_R$ was too low and was increased to 100,000. The results from these simulations are presented in Table 7. They show that the number of groundings is, on average, 50,887. This gives a probability of 0.51 groundings per year, which, compared to the accident statistics for the area, demonstrates a good agreement since five groundings were reported during a ten-year period (see Chapter 4.3). The average number of allisions is 721, which gives a probability of 0.007 allisions per year, or one allision every 139 years.
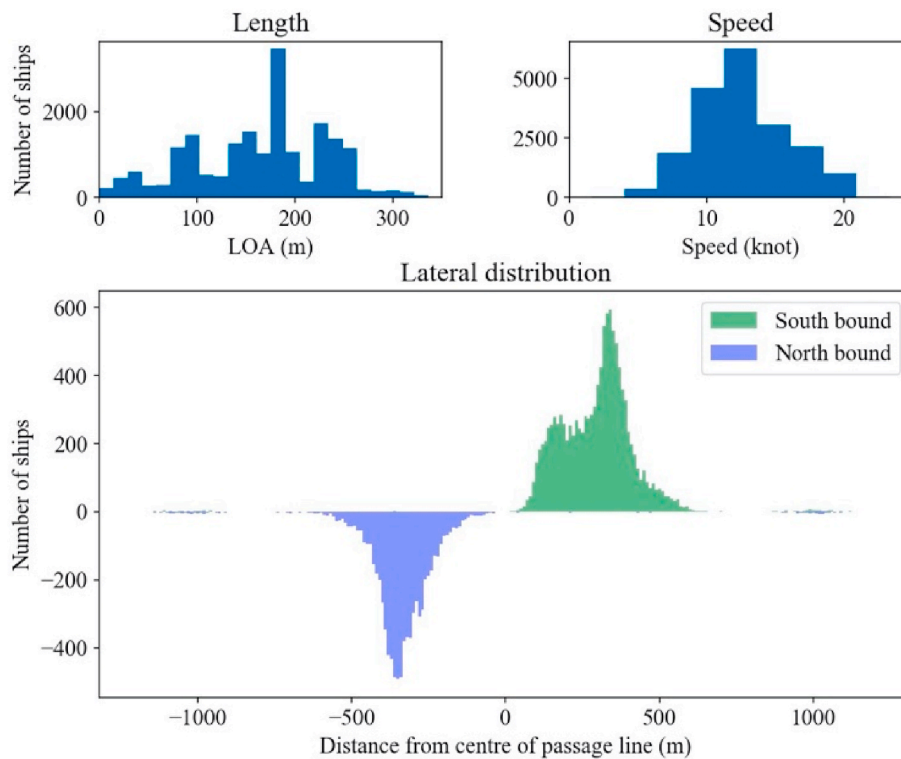
**Fig. 9.** Histograms of ship length, ship speed and lateral distribution of the marine traffic passing the Great Belt Bridge in 2019.
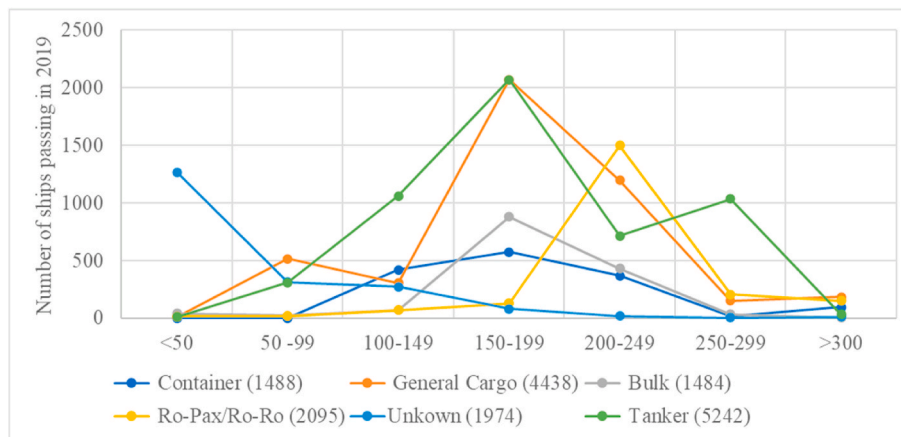


**Fig. 10.** Number of ships (y-axis) versus the length distribution of the ship types (x-axis) that passed under the Great Belt Bridge in 2019.

The 1,000-year allision energy shows some difference between the sets, but the deviation is less than five percent, which is acceptable. The average allision energy was calculated to 1,624 MJ, which represents a 178 m tanker with 57,870 DWT at ship speed 14.6 knots.

*6.2. Analysis of the duration time parameter*

Fig. 14 presents the results from an analysis of all simulations in simulation set 1A in Table 7, emphasising the influence from the parameter duration time in the three event categories. The green line represents the distribution of all simulations, while the blue dotted and the red dashed lines represent the distributions for the events that ended in grounding or allision accidents, respectively. The results show that the duration time in the drifting ship event had a small influence compared to the overall distribution and probability that lead to an allision. The duration time had a minor influence on the sharp turning

ship event results, but there was a large effect with regard to the miss of turning point event. Simulations with a longer duration time show a larger probability for grounding and allision accidents. The miss of turning point thus shows the highest probability for a grounding or allision accident. Fig. 15 presents the results from simulation set 1A to illustrate the paths of ships that collided with the bridge. Using the methodology presented in this study and these results, it is possible to propose and analyse mitigation actions that can help reduce or possibly avoid ship-bridge allisions.

*6.3. Analysis of two mitigation methods*

Two mitigations were analysed by simulation sets 5 and 6: reduction of maximum allowed ship speed and change of point where ships should make an earlier turn (change navigation path) to pass under the bridge, respectively. These two mitigation options were included to showcase

**Table 4**
List of ships modelled in the simulator and used in the case study; σ = standard deviation and μ = mean value.

| Ship type | Length (m) | Beam (m) | Draught (m) | Displacement (tonnes) | μ speed, (knots) | σ speed, (knots) | North going | South going |
|---|---|---|---|---|---|---|---|---|
| Container | 134 | 21 | 7.13 | 7,698 | 14.6 | 2.25 | 246 | 183 |
| Container | 170 | 26 | 9.3 | 23,027 | 14.3 | 2.81 | 540 | 315 |
| Container | 255 | 36 | 10.2 | 55,727 | 15.3 | 2.35 | 268 | 268 |
| General Cargo | 73 | 12 | 4.1 | 4,850 | 9.3 | 3.76 | 1,896 | 2,022 |
| General Cargo | 125 | 18 | 6.8 | 13,048 | 10.3 | 2.72 | 643 | 595 |
| General Cargo | 161 | 25 | 9.1 | 30,056 | 13.4 | 2.76 | 2,491 | 1,523 |
| Bulk | 169 | 27 | 9.23 | 55,459 | 11.5 | 1.78 | 790 | 339 |
| Bulk | 226 | 33 | 12.8 | 72,611 | 11.3 | 1.53 | 441 | 93 |
| Tanker | 79 | 13 | 4.8 | 6,538 | 10.2 | 1.97 | 136 | 131 |
| Tanker | 132 | 21 | 7.6 | 12,617 | 12.0 | 1.89 | 496 | 506 |
| Tanker | 178 | 28 | 9.9 | 57,870 | 12.6 | 1.70 | 1,545 | 374 |
| Tanker | 241 | 41 | 12 | 78,459 | 11.8 | 1.67 | 395 | 220 |
| Tanker | 260 | 45 | 11.8 | 164,820 | 11.8 | 2.00 | 481 | 365 |
| RoPax | 194 | 30 | 6.5 | 29,500 | 17.5 | 2.66 | 685 | 580 |
| RoPax | 252 | 31 | 6.5 | 36,256 | 16.9 | 1.66 | 485 | 462 |
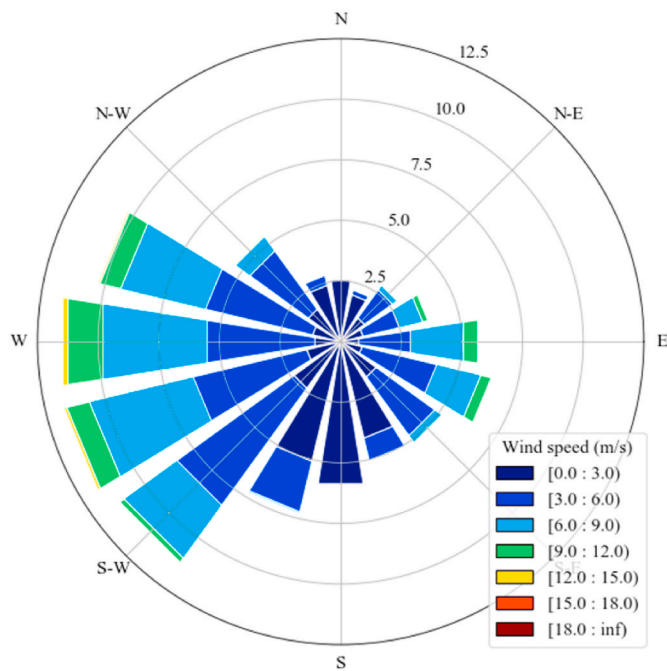


**Fig. 11.** Wind rose plot presenting the probability of wind speeds and wind directions. Data source: Copernicus Marine Service (2020), reanalysis-era5-single-levels.



**Fig. 12.** Current rose plot presenting the probability of current speeds and current directions. Data source: Copernicus Marine Service (2020), BALTICSEA_ANALYSIS_FORECAST_PHY_003_006.

possibilities with the methodology. They were designed based on similar ship fairway-bridge crossings. The results presented in Table 8 show that both these actions have a positive effect on reducing the number of accidents. The reason why the allision energy is significantly reduced is simply because many of the allision cases in set 1A did not occur for the miss of turning point event, which formerly gave the largest collision energies. It should be noted that the suggested mitigation actions have not been confirmed as realistic measures to be enforced in the area; however, with the methodology presented in this study, it is shown that they are worth investigating further, especially if marine traffic density and ship sizes continue to increase in the area. This is also supported by Pedersen et al. (2020), who recommended doing scenario-based simulations as a preparation for future changes and estimations of ship traffic situations and risk assessments.

### 6.4. Sensitivity analysis

A sensitivity study analysis was carried out to investigate how the probabilities and duration time parameters from the simulation sets
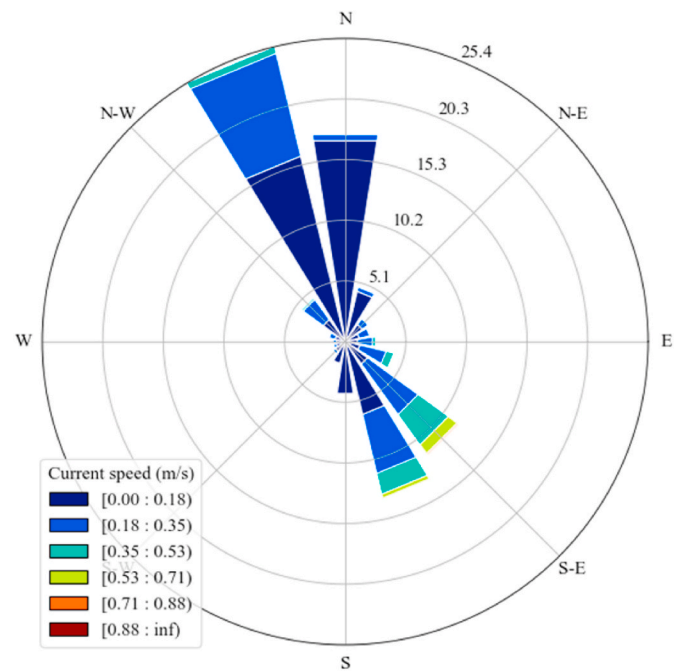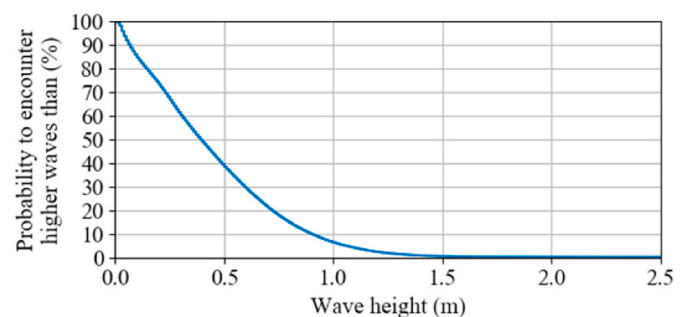


**Fig. 13.** Probability of occurrence of the wave height (m) at latitude 55.0–56.0° and longitude 10.4–11.4°. Data source: Copernicus Marine Service (2020), GLOBAL_REANALYSIS_WAV_001_032-TDS, period 1993 to 2018.

**Table 5**

Overview and definition of ten simulation sets run in the SEAMAN simulator. The parameters of the events and their details are presented in Chapters 4.1 and 4.2.

| ID | Seed | Description of event and simulation set |
|---|---|---|
| 1A | 0 | Drifting ship – probability: $0.65 \times 10^{-4}$; duration: $\sigma = 0.71$, $\iota = 0.021$, $\lambda = 0.69$ |
| 1B | 1 | Sharp turning ship – probability: $0.70 \times 10^{-5}$; duration: $\sigma = 1.2$, $\iota = 0.06$, $\lambda = 0.54$ |
| 1C | 2 | Miss of turning point – probability: $1.55 \times 10^{-5}$; duration: $\sigma = 0.015$, $\mu = 0.064$ |
| 2 | 0 | Drifting ship – probability: $0.91 \times 10^{-4}$; duration: $\sigma = 1.2$, $\iota = 0.1$, $\lambda = -0.4$ |
|  |  | The other events were modelled as defined in set 1 |
| 3 | 0 | Sharp turning ship – probability: $1.05 \times 10^{-5}$ |
|  |  | The other events were modelled as defined in set 1 |
| 4A | 0 | Miss of turning point – probability: $2.1 \times 10^{-4}$, duration: $\sigma = 0.047$, $\mu = 0.19$ |
|  |  | The other events were modelled as defined in set 1 |
| 4B | 0 | Miss of turning point – probability: $2.1 \times 10^{-4}$, duration for miss of turning point and the other events were modelled as defined in set 1 |
| 4C | 0 | Miss of turning point – duration: $\sigma = 0.047$ $\mu = 0.19$, probability for miss of turning point and the other events were modelled as defined in set 1 |
| 5 | 0 | Maximum ship speed: 12 |
|  |  | Event probabilities and durations as defined in set 1 |
| 6 | 0 | Longer straight navigation distance prior to the bridge |
|  |  | Event probabilities and durations as defined in set 1 |

**Table 6**

Results from simulation sets 1A, 1B and 1C with $Y_R = 10,000$.

| Id | Number of simulations | Number of groundings | Number of allisions | Maximum allision energy (MJ) | 1,000-year expected allision energy (MJ) |
|---|---|---|---|---|---|
| 1A | 395,770 | 5,165 | 59 | 2,308 MJ | 1,220 MJ |
| 1B | 395,770 | 5,214 | 67 | 2,315 MJ | 1,620 MJ |
| 1C | 395,770 | 5,065 | 56 | 1,967 MJ | 1,403 MJ |

affect the results, except for 1B, 1C, 5 and 6. Those sets were excluded because there was no need to include all the random seed simulation sets or the simulation sets that were defined for the mitigation study. The results are presented in Table 9.

Simulation sets 2 and 4 were based on the event statistics from the TSS Bornholmsgat area. Set 2 has a higher probability for drifting ship compared to simulation set 1A. This increased the number of groundings and allisions by about 25 percent. It did not, however, affect the 1,000-year allision energy. Set 3 has a 50 percent higher probability for sharp turning ship compared to simulation set 1A, which also showed a minor increase in the number of groundings and allisions but no influence on the 1,000-year allision energy.

For the miss of turning point in set 4A, the case study simulations show that this event has the largest influence and is, thereby, the most sensitive to the results. The increase of probability and duration were separated into 4B and 4C, to further investigate this event type and its effect on the result. An increase of only the event probability from $1.55 \times 10^{-4}$ to $2.1 \times 10^{-4}$ raised the number of allisions caused by miss of turning point from 0.25 percent per year to 0.32 percent per year and the expected 1,000-year allision energy by approximate 13 percent. However, an increase of the average duration from 0.064 h to 0.19 h affected the number of allisions by 2,900 percent and the expected 1,000-year allision energy by 251 percent. A comparison between the allision energy from sets 4C and 1A is illustrated in Fig. 16. An allision energy of approximately 4,268 MJ represents a 260 m tanker with 164,820 DWT at ship speed 14 knots or a larger tanker with 237,100 DWT at ship speed 12 knots.

The results in Fig. 16 show that some of the results are sensitive to the value of the parameter duration time, especially for the event miss of

turning point. This has not been studied in detail in similar investigations and models within the same research area (e.g. Goerlandt and Kujala, 2011; Hansen et al., 2013; van Dorp and Merrick, 2011). It is recommended that a stronger emphasis should be placed on this parameter in future work, as the manner which the duration time varies for different ship traffic areas, ship types and sizes should be studied in more depth.

## 6.5. Applicability of proposed methodology

In Chapter 4, the methods described in Chapter 3 were used to obtain event statistics in two areas. These areas have their differences when it comes to geography; however, they are both considered to be open sea and have well-defined sailing paths (partly regulated by TSS). Another area with well-defined sailing paths is the Kiel Canal; the methods to identify events were applied in this area, as well, but it was concluded that the methods were not applicable here. With the assumption that all the events led to accidents, and that all the accidents here were reported, the accidents from 2017 reported to IHS Fairplay and EMCIP were studied. The records give a higher frequency here for the loss of propulsion and rudder failure, but they are in the same magnitude as in the areas included in this paper. Although, it should also be noted that rudder failures in the accident records include more types of events than described in Chapter 3.2.

There are other events that were not investigated in the study that could result in an allision. One example of such an event is "cowboy ships", which was introduced by Pyman et al. (1983). The event defines ships that do not follow the intended navigation path and make turns at wrong locations in the fairway and traffic scheme. The cause behind the event could be crew/captains influenced by alcohol, malfunction of navigation aids, acts of terrorism, etc. This type of event was excluded from the study, since no method was found to model, identify and quantify the event. Another example of event that was not considered in the study is the category IV scenario proposed in Pedersen et al. (1995, 2020), which refers to a ship that makes an evasive manoeuvre because of another ship near a bridge. This event was not considered in the study for the same reasons as the cowboy ship event.

Compared to previous research and methods in, e.g., Ulusçu et al. (2009), van Dorp and Merrick (2011) and Goerlandt and Kujala (2011),
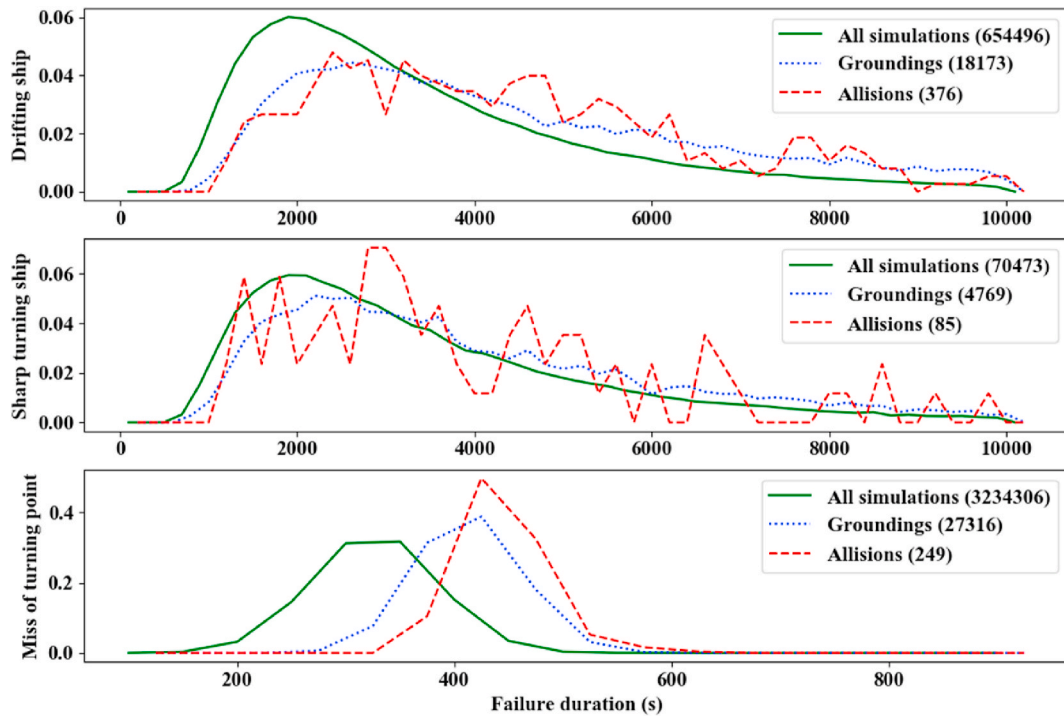
**Table 7**

Results from simulation sets 1A, 1B and 1C with $Y_R = 100,000$; number of allision accidents caused by D = drifting ship, ST = sharp turning ship, MTP = miss of turning point.

| Id | Number of simulations | Number of groundings | Number of allisions (D, ST, MTP) | Maximum allision energy (MJ) | 1,000-year expected allision energy (MJ) |
|---|---|---|---|---|---|
| 1A | 3,959,282 | 50,258 | 710 (376, 85, 249) | 3,221 | 1,667 |
| 1B | 3,959,282 | 51,198 | 722 (385, 97, 240) | 4,634 | 1,601 |
| 1C | 3,959,282 | 51,206 | 730 (395, 87, 248) | 2,708 | 1,605 |

**Fig. 14.** Analysis of the effects from the parameter duration time (simulation set 1A) on the probability density distributions for all simulations, groundings and accidents for the three studied events.
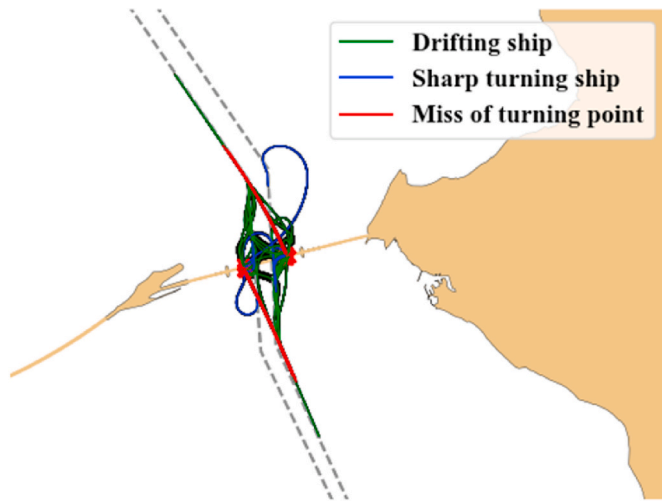


**Fig. 15.** Illustration of ten percent of the paths of ships from simulation set 1A that collided with the bridge. The green line represents the drifting ship event, the blue line the sharp turning ship event and the red line the miss of turning point event. (For interpretation of the references to colour in this figure legend, the reader is referred to the Web version of this article.)

the proposed methodology includes calculation of the hydrodynamic forces. It also contains methods for obtaining local event failure frequencies and durations. The study has demonstrated that the proposed methodology can be applied to allision case studies while other models in the literature often emphasize open sea and coastal areas. Finally, a difference between the proposed methodology and equation-based models (e.g., Pedersen, 1995, 2020) is that the probability and consequence of an event are analysed together instead of separately.

The proposed methodology can be used both to analyse the risk of existing bridges and in the planning phase of new bridges. The risk defined in Eq. (1) has the terms (accumulated) probability and

**Table 8**
Results from simulation sets 1A (reference), 5 and 6 with $Y_R = 100{,}000$; number of allision accidents caused by D = drifting ship, ST = sharp turning ship, MTP = miss of turning point.

| Id | Number of simulations | Number of groundings | Number of allisions (D, ST, MTP) | Maximum allision energy (MJ) | 1000-year expected allision energy (MJ) |
|---|---|---|---|---|---|
| 1A | 3,959,282 | 50,258 | 710 (376, 85, 249) | 3,221 | 1,667 |
| 5 | 3,959,282 | 32,003 | 436 (347, 89, 0) | 1,030 | 12 |
| 6 | 3,962,135 | 50,255 | 484 (402, 82, 0) | 2,258 | 22 |

**Table 9**
Results from simulation sets 1A (reference), 2, 3 and 4 with $Y_R = 100{,}000$; number of allision accidents caused by D = drifting ship, ST = sharp turning ship, MTP = miss of turning point.

| Id | Number of simulations | Number of groundings | Number of allisions (D, ST, MTP) | Maximum allision energy (MJ) | 1000-year expected allision energy (MJ) |
|---|---|---|---|---|---|
| 1A | 3,959,282 | 50,258 | 710 (376, 85, 249) | 3,221 | 1,667 |
| 2 | 4,221,089 | 65,516 | 985 (651, 85, 249) | 3,221 | 1,667 |
| 3 | 3,994,525 | 54,268 | 800 (376, 175, 249) | 3,221 | 1,667 |
| 4A | 5,169,542 | 1,020,580 | 27,954 (376, 85, 27,493) | 4,822 | 4,268 |
| 4B | 5,169,542 | 60,662 | 777 (376, 85, 316) | 3,221 | 1,880 |
| 4C | 3,959,282 | 748,053 | 20,606 (376, 85, 20,145) | 5,054 | 4,179 |
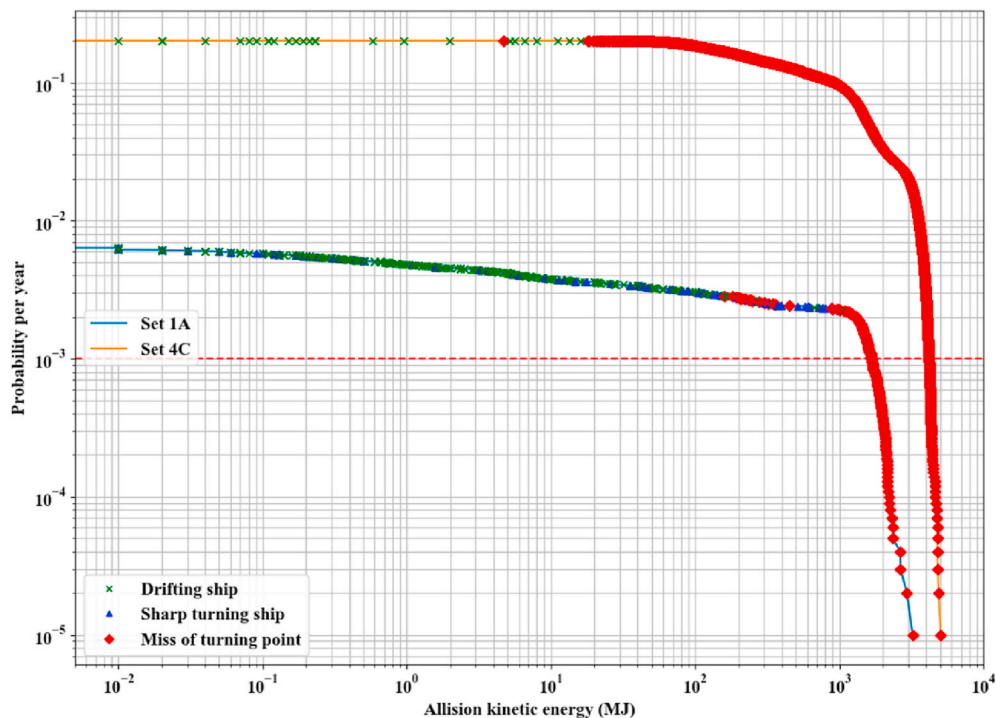
**Fig. 16.** A log-log diagram presenting the probability of allision energy for the simulation sets 1A and 4C for the three studied events. The allision energy is calculated in accordance with Eq. (4).

consequence, which were also analysed for each simulation case in the methodology. This definition of risk and the way to present accumulated probability in Fig. 16 is similar to Johansen and Askeland (2019) who used an FN-curve as the design criterion for bridge design. Note that the FN-curve has the number of fatalities on the *x*-axis and Fig. 16 has the allision energy. In future research, the allision energy could be translated to damages to the bridge and thereafter converted to number of fatalities.

## 7. Conclusions

The study presented a methodology using AIS data, a ship manoeuvring simulator and the Monte Carlo method to calculate the accident probabilities in marine traffic near bridges spanning over wide waterways. The methodology was verified in a case study on grounding accidents, and its wider applicability was presented in a case study where the probability of ship-bridge allisions was calculated. With the proposed methodology, ships and traffic situations that were over-represented in the failure event analyses in the case study's marine traffic area were numerically shown, and mitigation actions were proposed that can reduce the probability of ship-bridge allisions. Ships that represent the 1,000-year allision energy were identified, which can be used as target ships in bridge structural strength assessments and whose kinetic energy impact a bridge must withstand.

An event-based approach was proposed for the identification of events that should be simulated and analysed if they can lead to a maritime accident. This is based on an analysis of AIS data of the traffic separation scheme of the area of interest. Event detection criteria for three events, drifting ship, sharp turning ship and miss of turning point, were proposed. The marine traffic areas Great Belt VTS and TSS Bornholmsgat were analysed to estimate the event frequency. The results were compared with results in Rasmussen et al. (2012), and there was good agreement for the drifting ship and miss of turning point events. For the sharp turning ship event, too few events in the AIS data were found to form representative statistical conclusions.

The Great Belt VTS area was used in a verification study that

confirmed that the methodology could predict the probability of ship groundings corresponding to the accident statistics from the past ten years in the same area. It was concluded that the presented methodology can be used to simulate and analyse traffic situation schemes in costal waterways to calculate the probability that a ship accident will occur.

The ship-bridge allision case study of the Great Belt Bridge showed in a sensitivity study that the parameter duration time of an event has a large influence on the results. It is thus recommended to carry out a parametric sensitivity study of this parameter. In the current case study, it was shown to have a relatively large influence, especially on the miss of turning point event and the subsequent way the ship's situation in the simulator runs evolved.

A sensitivity study of the number of simulated traffic years showed that 100,000 traffic years were required to satisfy the convergence criterion defined in the study. The probability for a ship allision against the Great Belt Bridge was calculated to be 0.007. An analysis of all ship-bridge allision cases showed that it was dominated by the drifting ship event. The expected allision energy for the 1,000-year allision was calculated to be 1,624 MJ, which can be represented by a 178 m tanker with 57,870 DWT and ship speed 14.6 knots. However, if the duration of the event miss of turning point was increased to the same duration as in the TSS Bornholmsgat the expected allision energy for a 1,000-year allision was increased to 4,268 MJ, which can be represented by a 260 m tanker with 164,820 DWT at ship speed 14 knots or a larger tanker with 237,100 DWT at ship speed 12 knots.

Two mitigation actions were studied: change of the traffic separation scheme and limitation of the ship speed. Both of these actions will give the crew more time to act and react in case they lose the manoeuvrability of the ship; hence, the probability of an allision was reduced.

The methodology presented in the study and its results show that it can be applied either in the planning phase of a new bridge over a waterway if the AIS data in the area are known, or in the assessment of marine traffic situations near existing bridges where the marine traffic may have changed since they were designed and built. The methodology is not limited to ship-bridge allisions; it can also be used to assess the probability of collisions with other infrastructures offshore or other

marine accidents, such as ship groundings.

The event failure probability can be included directly in other navigational risk assessment methods to assess the risk of collision when vessels are close to each other. In future research, the methodology should be developed to include multiple ships in the simulation models, and implement active decision support how other ships can meet and interact more safely in fairways which high traffic density. This extension of the simulation methodology would offer a possibility to simulate and analyse the probabilities and consequences of ship-ship collisions.

## CRediT authorship contribution statement

**Axel Hörteborn:** Conceptualization, Methodology, Software, Validation, Formal analysis, Data curation, Investigation, Writing – original draft, Funding acquisition. **Jonas W. Ringsberg:** Conceptualization, Writing – review & editing, Supervision.

## Declaration of competing interest

The authors declare that they have no known competing financial interests or personal relationships that could have appeared to influence the work reported in this paper.

## Acknowledgements

## References

AASHTO, 2009. Guide Specifications and Commentary for Vessel Collision Design of Highway Bridges, second ed. American Association of State Highway and Transportation Officials (AASHTO), U.S.A., ISBN 9781560514268

Andreasson, H., Källman, M., Liljenberg, H., Olofsson, H., Trägårdh, P., Wilske, E., 2005. Design for safe and efficient LNG Carriers. In: Proceedings of SNAME Maritime Technology Conference and Expo and Ship Production Symposium 2005. Curran Associates, Inc., Houston, Texas, USA, pp. 413–422, 19-22 October 2005. U.S.A.

Budak, G., Beji, S., 2020. Controlled course-keeping simulations of a ship under external disturbances. Ocean Eng. 218, 108126 https://doi.org/10.1016/j.oceaneng.2020.108126.

CEN, 2006. Eurocode 1 - Actions on Structures - Part 1-7: General Actions - Accidental Actions. European Standard EN 1991-1-7. European Committee for Standardization, Brussels, Belgium.

Chen, P., Huang, Y., Mou, J., van Gelder, P.H.A.J.M., 2019. Probabilistic risk analysis for ship-ship collision: state-of-the-art. Saf. Sci. 117 (1), 108–122. https://doi.org/10.1016/j.ssci.2019.04.014.

Chillcce, G., el Moctar, O., 2018. A numerical method for manoeuvring simulation in regular waves. Ocean Eng. 170 (1), 434–444. https://doi.org/10.1016/j.oceaneng.2018.09.047.

Copernicus Marine Service, 2020. Copernicus Marine Service [cited 2020 October 19]. Available from: https://marine.copernicus.eu/.

DMA, 2020. AIS Data from the Danish Maritime Authority [cited 2020 October 19]. Available from: https://www.dma.dk/SikkerhedTilSoes/Sejladsinformation/AIS/Sider/default.aspx.

El-Naby, R.M.A., Gamal, A.A., El-Sayed, T.A., 2014. Controlling the demolition of existing structures: an approach to analyze the collapse of the World Trade Center North Tower WTC1. Int. J. Civ. Eng. Technol. 5 (11), 57–78.

EMCIP, 2020. EMCIP Public Dashboard [cited 2020 October 19]. Available from: https://portal.emsa.europa.eu/emcip-public/#/dashboard.

EMSA, 2019. Annual Overview of Marine Casualties and Incidents 2019 [cited 2020 October 19]. Available from: http://www.emsa.europa.eu/news-a-press-centre/external-news/item/3734-annual-overview-of-marine-casualties-and-incidents-2019.html.

Fairplay, I.H.S., 2020. Sea-web Casualty & Events [cited 2020 October 19]. Available from: https://maritime.ihs.com/.

Fujii, Y., 1983. Integrated study on marine traffic accidents. Iabse Colloquium Copenhagen 1983 - Ship Collision With Bridges offshore Struct. 42, 91–98.

Furnes, O., Amdahl, J., 1980. Computer simulation study of offshore collisions and analysis of ship platform impacts. Norweg. Marit. Res. 8 (1), 2–12.

Gluver, H., Olsen, D., 1998. Current practice in risk analysis of ship collisions to bridges. In: Gluver, H., Olsen, D. (Eds.), Proceedings of the International Symposium on Advances in Ship Collision Analysis, Copenhagen, Denmark, 10-13 May 1998. Balkema Publishers, The Netherlands, pp. 85–96.

Goerlandt, F., Kujala, P., 2011. Traffic simulation based ship collision probability modeling. Reliab. Eng. Syst. Saf. 96 (1), 91–107. https://doi.org/10.1016/j.ress.2010.09.003.

Hansen, M.G., Randrup-Thomsen, S., Askeland, T., Ask, M., Skorpa, L., Hillestad, S.J., Veie, J., 2013. Bridge crossings at Sognefjorden–ship collision risk studies. In: Amdahl, J., Ehlers, S., Leira, B.J. (Eds.), Collision and Grounding of Ships and Offshore Structures. ICCGS2013: Proceedings of the 6th International Conference in Collision and Grounding of Ships and Offshore Structures (ICCGS), Trondheim, Norway, 17-19 June 2103. CRC Press/Taylor and Francis Group, U.K., pp. 9–18

Harris, C.R., Millman, K.J., van der Walt, S.J., Gommers, R., Virtanen, P., Cournapeau, D., Wieser, E., Taylor, J., Berg, S., Smith, N.J., Kern, R., Picus, M., Hoyer, S., van Kerkwijk, M.H., Brett, M., Haldane, A., Fernández del Río, J., Wiebe, M., Peterson, P., Gérard-Marchant, P., Sheppard, K., Reddy, T., Weckesser, W., Abbasi, H., Gohlke, C., Oliphant, T.E., 2020. Array programming with NumPy. Nature 585 (1), 357–362. https://doi.org/10.1038/s41586-020-2649-2.

Hassel, M., Asbjørnslett, B.E., Hole, L.P., 2011. Underreporting of maritime accidents to vessel accident databases. Accid. Anal. Prev. 43 (6), 2053–2063. https://doi.org/10.1016/j.aap.2011.05.027.

Hollnagel, E., Woods, D.D., Leveson, N., 2006. Resilience Engineering: Concepts and Precepts. CRC Press/Taylor and Francis, Boca Raton.

Hörteborn, A., Ringsberg, J.W., Svanberg, M., Holm, H., 2019. A revisit of the definition of the ship domain based on AIS analysis. J. Navig. 72 (3), 1–18. https://doi.org/10.1017/S0373463318000978.

IALA, 2014. Welcome to the IWRAP Mk2 Wiki Site [cited 2020 October 19]. Available from: https://www.iala-aism.org/wiki/iwrap/.

IMO, 2002. Report of the Maritime Safety Committee on its Seventy-Sixth Session. Annex 6, Resolution MSC. 137 (76) - Standards for Ship Manoeuvrability. IMO Report 76/23. International Maritime Organization, U.K.

Johansen, I.L., Askeland, T., 2019. Risk acceptance criteria for extreme fjord crossings. In: IABSE Symposium, Guimaraes 2019: towards a Resilient Built Environment Risk and Asset Management - Report. International Association for Bridge and Structural Engineering (IABSE), ISBN 978-3-85748-163-5, pp. 1402–1409.

Källström, C.G., Ramzan, F.A., 1985. The use of hybrid model tests and computer simulations for offshore installations. In: Presented at the IFAC/IFIP International Conference on "Automation for Safety in Shipping and Offshore Petroleum Operations. " Amsterdam North-Holland, Trondheim, Norway, ISBN 978-0-444-70101-5, pp. 41–50, 1986.

Kaneko, F., 2012. Models for estimating grounding frequency by using ship trajectories and seabed geometry. Ships Offshore Struct. 7 (1), 87–99. https://doi.org/10.1080/17445302.2011.594572.

Lu, Z., Amdahl, J., Storheim, M., 2016. A new approach for coupling external dynamics and internal mechanics in ship collisions. Mar. Struct. 45 (1), 110–132. https://doi.org/10.1016/j.marstruc.2015.11.001.

Macduff, T., 1974. The probability of vessel collisions. Ocean Ind. 9 (9), 144–148.

Montewka, J., Goerlandt, F., Kujala, P., 2012. Determination of collision criteria and causation factors appropriate to a model for estimating the probability of maritime accidents. Ocean Eng. 40 (1), 50–61. https://doi.org/10.1016/j.oceaneng.2011.12.006.

Ottosson, P., 1994. Mathematical models in PORTSIM. In: Roberts, G.N., Pourzanjani, M. M.A. (Eds.), MCMC'94: Proceedings of the 3rd International Conference Manoeuvring and Control of Marine Craft. Southampton Institute, ., pp. 177–196. Southampton, U.K., 7-9 September 1994. U.K.

Ottosson, P., Bystrom, L., 1991. Simulation of the dynamics of a ship manoeuvring in waves. Trans. - Soc. Nav. Archit. Mar. Eng. 99 (1), 281–298.

Pedersen, P.T., 1995. Collision and grounding mechanics. In: WEMT'95: Proceedings of Ship Safety and Protection of the Environment - from a Technical Point-of-View, 1. Danish Society of Naval Architecture and Marine Engineering, Denmark, pp. 125–157. Copenhagen, Denmark, 17-19 May 1995.

Pedersen, P.T., Chen, J., Zhu, L., 2020. Design of bridges against ship collisions. Mar. Struct. 74 (1), 102810 https://doi.org/10.1016/j.marstruc.2020.102810.

Psarros, P., Skjong, R., Eide, M.S., 2010. Under-reporting of maritime accidents. Accid. Anal. Prev. 42 (2), 619–625. https://doi.org/10.1016/j.aap.2009.10.008.

Pyman, M.A.F., Austin, J.S., Lyon, P.R., 1983. Ship/platform collision risk in the UK sector. Iabse Colloquium Copenhagen 1983 - Ship Collision With Bridges offshore Struct. 42, 145–152.

Rasmussen, F.M., Glibbery, K.A.K., Melchild, K., Hansen, M.G., Jensen, T.K., Lehn-Schiøler, T., Randrup-Thomsen, S., 2012. Quantitative assessment of risk to ship traffic in the Fehmarnbelt fixed link project. J. Polish Saf. Reliab. Assoc. 3 (1), 123–134.

Raymond, E.S., 2019. AIVDM/AIVDO Protocol Decoding [cited 2020 October 19]. Available from: https://gpsd.gitlab.io/gpsd/AIVDM.html.

Sha, Y., Amdahl, J., 2019. A simplified analytical method for predictions of ship deckhouse collision loads on steel bridge girders. Ships Offshore Struct. 14 (1), 121–134. https://doi.org/10.1080/17445302.2018.1560881.

Sjofartsdirektoratet, 2020. Ulykkesstatistikk – Sjøfartsdirektoratet [cited 2020 October 19]. Available from: https://www.sdir.no/sjofart/ulykker-og-sikkerhet/ulykkesstatistikk/.

Svanberg, M., Santén, V., Hörteborn, A., Holm, H., Finnsgård, C., 2019. AIS in maritime research. Mar. Pol. 106, 103520 https://doi.org/10.1016/j.marpol.2019.103520.

Uluscu, Ö.S., Özbaş, B., Altıok, T., Or, İ., 2009. Risk analysis of the vessel traffic in the strait of Istanbul. Risk Anal. 29 (10), 1454–1472. https://doi.org/10.1111/j.1539-6924.2009.01287.x.

van Dorp, J.R., Merrick, J.R.W., 2011. On a risk management analysis of oil spill risk using maritime transportation system simulation. Ann. Oper. Res. 187 (1), 249–277. https://doi.org/10.1007/s10479-009-0678-1.

Wei, Z., Xie, X., Zhang, X., 2020. AIS trajectory simplification algorithm considering ship behaviours. Ocean Eng. 216, 108086 https://doi.org/10.1016/j.oceaneng.2020.108086.

Yu, Z., Amdahl, J., Storheim, M., 2016. A new approach for coupling external dynamics and internal mechanics in ship collisions. Mar. Struct. 45 (1), 110–132. https://doi.org/10.1016/j.marstruc.2015.11.001.

Zhao, L., Shi, G., 2019. A trajectory clustering method based on Douglas-Peucker compression and density for marine traffic pattern recognition. Ocean Eng. 172 (1), 456–467. https://doi.org/10.1016/j.oceaneng.2018.12.019.